

WETTABILITY AND MECHANICAL STRENGTH OF MODIFIED NAFION[®] NANOCOMPOSITE MEMBRANE FOR FUEL CELL

R. SIGWADI^a, M. DHLAMINI^b, T. MOKRANI^a, F. NEMAVHOLA^{c*}

^a*Department of Chemical Engineering, University of South Africa, Private Bag X6, Florida, 1710, South Africa*

^b*Department of Physics, University of South Africa, Private Bag X6, Florida, 1710, South Africa*

^c*Department of Mechanical Engineering, University of South Africa, Private Bag X6, Florida, 1710, South Africa*

Synthesised water-retaining mesoporous zirconia nanoparticles were used to modify Nafion[®] membrane. This experiment was conducted to enhance the mechanical strength and hydrophilicity of Nafion[®] membrane for high temperature fuel cell applications. Recast methods were used to prepare a nanocomposite membrane with 10wt% of zirconia nanoparticles. The water contact angle (wettability) and water uptake of the composited membrane were measured. The modified membranes with zirconia nanoparticles showed a significant improvement in water uptake and contact angle leading to enhanced hydrophilicity when compared to unmodified hydrophobic Nafion[®] membrane. This shows the potential for use as electrolytes in fuel cell applications. The X-ray diffraction (XRD) results show a modified Nafion[®] membrane with zirconia nanoparticles increases the crystallinity of the membrane. Furthermore, Scanning Electron Microscopy (SEM), Fourier transform infrared spectra (FTIR), Thermogravimetric analysis (TGA), AFM and tensile strength were used to observe the morphology, thermal decomposition, structure and mechanical and physical properties of the nanocomposite membrane. SEM results show good distribution of zirconia nanoparticles within the membranes. In addition, TGA results of modified membranes showed the improvement in thermal stability.

(Received July 14, 2017; Accepted November 22, 2017)

Keywords- Zirconium oxide, Wettability; Mechanical strength, Nanoflower, nanocomposite

1. Introduction

Fuel cell technology is an environmentally friendly energy resource, which generates electricity while removing water as by-product. It can operate using hydrogen and methanol as fuel, but there are limitations, as cells will need electrolytes that prevent fuel crossover while will conducting. Proton exchange membrane fuel cells (PEMFCs) have been recognised as the most promising power source for electric vehicles because they are emission-free and have relatively high power generation efficiency [1]. The Nafion[®] membrane is currently the most popular on account of its superior mechanical and chemical stability and good electrochemical performance [2], robust structure and excellent proton conductivity in hydrated states [3]. The microstructure of Nafion[®] membrane consists of three components: hydrophobic fluorocarbon backbone, hydrophilic ionic clusters of sulfonic acid groups (proton exchange sites) and an interfacial component [4, 5]. The superselectivity of Nafion[®] and its chemical and thermal stability are ascribed to its structure [6]. The proton migration within the Nafion[®] membrane depends on water

* Corresponding author: fulufhelo.masithulela@gmail.com

uptake [1]. At high temperatures, pristine Nafion[®] membrane has disadvantages such as loss of water by evaporation resulting in irreversible mechanical damage and lower proton conductivity at low relative humidity, which limit operations at high temperatures. In addition, the application of Nafion[®] membrane in fuel cells is further limited by methanol permeability, which results in the release of CO damaging the catalytic side of fuel cells. High temperature operations are performed in order to maintain reasonable proton conductivity, good mechanical stability, enhance reaction kinetics at both electrodes, improve carbon monoxide tolerance of the platinum catalyst at the anode and simplify heat and humidity management of polymer electrolyte membrane (PEM) fuel cells [7]. increases the binding energy of water [8]. Due to its molecular structure, Nafion[®] tends to shrink when relative humidity decreases and swell in water [9]. Moreover, the mechanical properties of the membrane are affected by changes of temperature and water content [10]. The researches worked on developing a modified Nafion[®] membrane using an inorganic filler, to store water in the membrane, which does not evaporate at higher temperatures on account of the electrostatic attraction in the electrical double layer [11], anti-swelling and hydrophilic properties [12-15]. Furthermore, membrane strength and performance increase as the specific surface area of the inorganic component increases [16], in fact the use of inorganic material improves the electrical, mechanical, and optical properties of any compound when surface area is increased [17]. Modified membranes with inorganic fillers such as silica (SiO₂) [11, 18], titanium dioxide (TiO₂) [18, 19], zirconium oxide (ZrO₂) [18, 19], heteropoly-acids [20] and zeolites [21] were used to facilitate proton conductivity at high temperatures and a low Relative Humidity (RH), water management, mechanical properties and to change pore and channel structures. [22-25]. estructured hydrophilic channels were composed of water-retaining pendant sulfonic acid groups, which may be due to the degree of acidity of the nanofiller [26]. Furthermore, when a membrane is modified by inorganic particles, mechanical properties such as tensile strength, modulus or stiffness are improved [27, 28]. Zirconia oxide (ZrO₂) is a metal oxide that is stable at high temperatures and has high mechanical properties [29]. ZrO₂ is obtained in three different crystal phases at ambient pressure, monoclinic, tetragonal and cubic, that strongly influence the catalyst's activities and selectivity [30, 31]. In this paper, the incorporation of zirconia nanoparticles within the Nafion[®] membrane was prepared by recast method, in order to enhance the wettability and mechanical strength of electrolytes for proton exchange membrane fuel cells (PEMFCs). The effects of ZrO₂ nanoparticles on the recast membrane on hydrophilicity and mechanical properties under tensile test and water contact angle were observed.

2. Method

2.1. Preparation of ZrO₂ nanoparticles

ZrO₂ nanoparticles were prepared by precipitation method, and zirconium oxychloride hydrate (ZrOCl₂·8H₂O) and sodium hydroxide (NaOH) were used as starting materials. 0.2M ZrOCl₂·8H₂O were dissolved in 50 ml deionised water. NaOH [2N] solution was added dropwise to the ZrOCl₂·8H₂O (50 ml) solution and stirred continuously for 45 minutes. The precipitate was covered with foil and put in an oven at 80 °C temperatures for 24 hours, after which it was then centrifuged and washed many times with deionised water until Cl⁻ was no longer detected. It was then dried at 80 °C, calcinated at 600 °C for 4 hours and labelled as Zr-80.

2.2. Preparation of nanocomposite membranes.

The nanocomposite membranes were prepared using 5 % Nafion[®] solution as the standard material for reference. Nafion[®] solution (10ml) was mixed with N, N-dimethylformamide (DMF) (20ml) to replace solvents. 10wt % of Zr-80 nanoparticles were added to the Nafion[®]/ DMF solution and stirred at room temperature for 2 hours, then ultrasonised for 30 minutes [32]. The resulting solution was poured onto a piece of flat glass, and placed in an oven at 80 °C for 12 hours to remove solvent, and finally heated up to 160 °C for 30 minutes. The membranes were then removed by peeling them off the glass plate. Before conducting any measurement, all membranes were placed in deionised water for 12 hours. The thicknesses of the membrane were measured with a digital micrometer (0.18 cm). Each thickness was measured at an average of 3-7 reading at different positions on membrane and this process was repeated twice on each membrane in order to obtain the average value.

2.3. Characterizations

The X-ray diffraction (XRD) analysis was performed using a Philips X-ray diffraction with Cu K radiation source. The analysed material was finely ground, homogenised, and average bulk composition determined. Samples were scanned in a continuous mode from 10° - 90° with a scanning rate of 0.026 (degree) / 1 (sec). The thermal properties of the samples and its characteristics were studied by thermal gravimetric analysis (TGA) under nitrogen flow. TGA data was obtained using model STA (Simultaneous Thermal Analyzer) 1500 (supplied by Rheometric Scientific Ltd, UK), over nitrogen at a heating rate of 10 °C/min from 28 °C to 1000 °C. Fourier Transform Infrared (FT-IR) investigated the changes in the chemical structure of the membrane. Scanning Electron Microscopy (SEM) images were obtained on a Hitachi x650. Electronic techniques were based on the interaction of the sample with electrons which resulted in a secondary effect that is detected and measured. Dynamic Light Scattering (DLS) measurements and Transmission electron microscopy (TEM) were used to observe the surface area. The surface morphology of nanocomposite membranes and roughness analysis was measured by Atomic force microscopy (AFM).

2.4. Tensile Test

The uniaxial mechanical properties of nanocomposite membranes and recast membrane were captured using a uniaxial testing system. The length, width and thickness of samples were measured using a Vernier caliper and recorded prior to testing. The testing area of the membrane samples were 4 mm x 10 mm in dimension. To allow clamping area, the samples were prepared in such a way that they could clamped both sides and still allow for a testing area of 4 mm x 10 mm. The thickness of 0.18 cm of the nanocomposite membrane was used in analyzing the stress applied to the sample. The membranes were soaked in water for 24 hours, and wet tested. Then the membranes were dried in a vacuum oven at 80 °C for 24 hours and tested as dry test. The tensile strength of modified Nafion® membranes was measured using CellScale Ustretch device, dried at 25 °C and wet at 34 °C with an actuator speed of 5 mm per min.

2.5. Water Contact Angle Measurements

The hydrophilicity of the membrane surfaces was performed under contact angles measurement (Phoenix 300 contact angle analyser (Surface Electro Optics Co.,Korea) instrument equipped with a video system. Membranes were cut into strips and mounted on glass slides for analysis. A droplet of deionized water (0.16 µL) was deposited on the surface of the membranes at ambient temperature by placing the tip of the syringe close to the sample surface, with all images being captured on camera. The measurement was repeated 10 times at different surfaces of membrane to obtain an average value. Before the water droplet attached to the sample surface, the wetting process was recorded until no significant change at the surface was observed any more [33].

2.6. Water uptake measurements

The membranes was immersed in deionized water for 24 hours, blotted with a paper towel and then measured as wet mass percentage. The membranes were then dried in a vacuum oven at 80°C for 24 hours and measured. The water uptakes of the nanocomposite membranes and recast Nafion® membrane were calculated from the equation:

$$Wup() = \frac{(m_{wet} - m_{dry})}{m_{dry}} * 100 \quad (2)$$

Where m_{wet} and m_{dry} are the weights of fully hydrated and the anhydrous membranes, respectively.

3. Results and discussion

3.1. Dynamic Light Scattering (DLS) measurements

The resulting particle size distribution is shown in Figure 1. As illustrated in Figure 1, DLS measurements of a sample synthesized at 80 °C for 24 hours agree with TEM in regard to particle size distribution. TEM measurements (insert) in Figure 1 show the real particle size while

DLS measures the hydrodynamic radius of the synthesized particles [34]. Figure 1(a) insert picture, shows that the nanoparticles aggregate in the form of 10-20 nm diameter. Results from light scattering measurements in Figure 1 show that the average particle size is 345 nm and that the particle size distribution is narrow. This means particles in Figure 1(b) are also 3.40 μm , respectively, with slightly broadened particle size distribution. The nanocomposite mean particle size is bigger than the zirconia nanoparticles on the surface area, which has resulted in a slightly broadened particle size distribution in Figure 1(b). This result indicates that the nanocomposite were slightly agglomerated, which may result from the synthesis procedure.

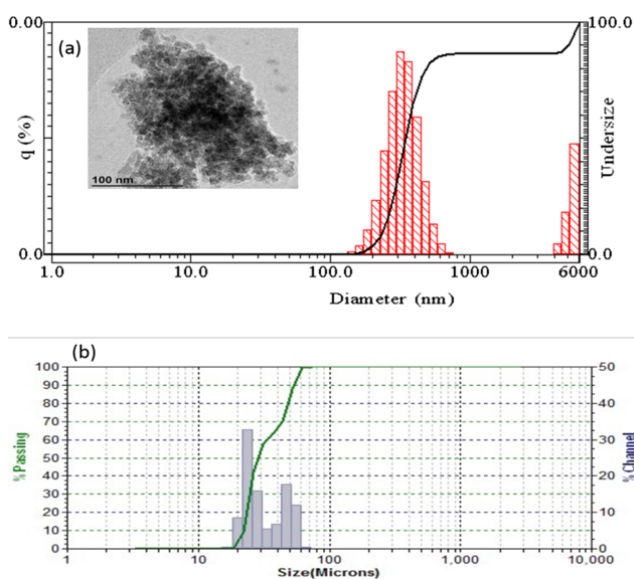


Fig. 1. Dynamic Light Scattering (DLS) of (a) Zr-80 nanoparticles, (insert) TEM micrograph of Zr-80 nanoparticles. (b) Nafion[®]/Zirconia nanocomposite.

3.2. Morphology

The SEM image of the Nafion[®]/Zr-80 nanocomposite membrane and Zr-80 nanoparticles (insert) are shown in Fig. 2. The cross-section and surface morphologies of the modified membrane show that zirconia nanoparticles are well distributed within the membrane matrix that confirm XRD results. Fig. 2 clearly shows the white particles within the Nafion[®] membrane indicating zirconia nanoparticles have been successfully dispersed by the recast method without any aggregation due to their compatibility. The cross-section of nanocomposite membranes shows good dispersion of zirconia across the thickness of the membrane without macroscopic void, space and cracks. The red arrow in Figure 2 shows the microscopic porosity within the modified membrane with inorganic nanoparticles that enhance the membrane's water uptake [35]. It is notable in Figure 2 (yellow circles and arrow) that zirconia nanoparticles are uniformly distributed through the whole membrane with coarser pores in the interlayer membrane [36]. The insert image shows the nanoparticles aggregated in the form of nanoflowers with a diameter of less than 100 nm. Moreover, the distribution of inorganic filler within the modified membrane has been identified by tapping mode atomic force microscopy [37]. The amplitude and topography images measured in tapping mode of Nafion[®]/Zr-80 nanocomposites membranes are shown in Figure 3. The modified membranes reveal the presence of ZrO₂ nanoparticles on the surface of the Nafion[®] membrane showing roughness of 60.8 nm. In Figure 3 (b), the structure of the nodules can be seen on the membrane's surface. From the topography and amplitude images, we can clearly see significant changes in the surface morphology with the addition of ZrO₂, which indicates the strong interaction of filler material within the Nafion[®] matrix [38]. The increased surface roughness of modified Nafion[®] nanocomposite membranes improves the contact between the electrodes [39].

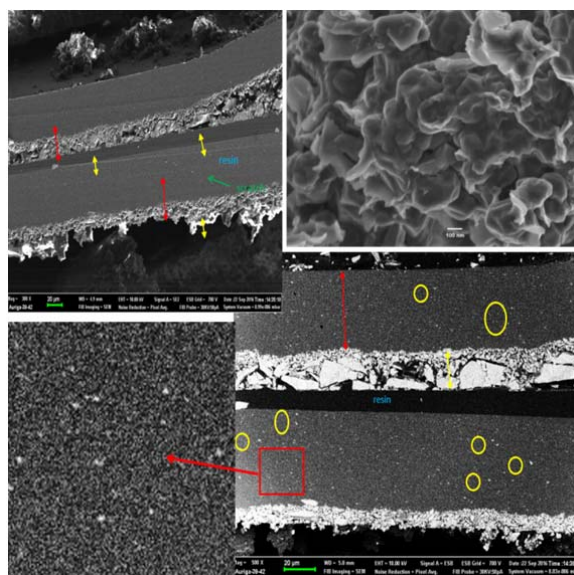


Fig. 2. SEM micrograph of Nafion[®]/Zr-80 nanocomposite membrane, (insert) SEM micrograph of Zr-80 nanoparticles

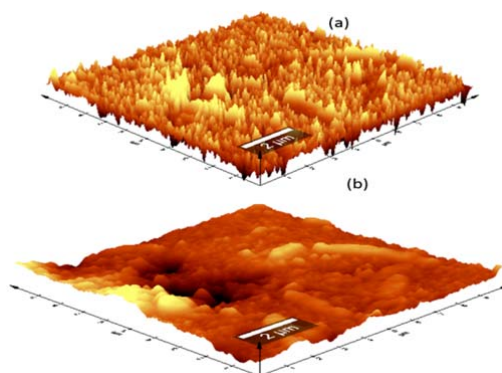


Fig. 3. Atomic force microscopy (AFM) (a) amplitude image (b) topography measured in tapping mode of the modified membranes

3.3. Tensile Tests

Uniaxial force was applied to recast Nafion[®] and Nafion[®]/Zr-80 nanocomposite membranes. The stress-strain curve was used to determine the elastic modulus of nanocomposite membranes. As shown in Figure 4, the elastic modulus of elasticity of dry Nafion[®]/Zr-80 nanocomposite membrane is slightly lower than that of dry recast Nafion[®]. Similarly, the elastic modulus of elasticity of wet Nafion[®]/Zr-80 nanocomposite membrane is lower than that of wet recast Nafion[®]. This may be due to poor dispersion of the inorganic filler within the polymer [40]. Figure 5 shows that the elastic modulus of dry recast Nafion[®] is 1.19% higher than that of the dry Nafion[®]/Zr-80 nanocomposite membranes. Similarly, elastic modulus of wet recast Nafion[®] is 31.24% higher than the wet Nafion[®]/Zr-80 nanocomposite membranes. The strength of Nafion[®]/Zr-80 nanocomposite membrane is greatly affected by moisture content when compared to recast Nafion[®], because the inorganic nanofiller stores water within the membrane [12, 13]. Even when the effect of moisture is detected in the recast Nafion[®] membrane, it is not as great as in the Nafion[®]/Zr-80 nanocomposite membrane. Figure 4 (e) shows improvement in the secant modulus

of dry Nafion[®]/ Zr-when compared to the recast membrane. This is due to the incorporation of zirconia nanoparticles that retain water and enhance mechanical strength of Nafion[®] membranes, revealing the close bonding between zirconia nanoparticles and Nafion[®] membrane through self-assembly. This improvement of membrane rigidity demonstrates that the zirconia nanoparticles stabilise the structure of modified membranes, and are a potential restriction to humidity-generated stress when the membrane is used as an electrolyte in fuel cells applications. Hence, it is observed that the recast Nafion[®] membrane in wet state has a higher modulus of elasticity and tensile strength when compared to Nafion[®]/Zr-80 due to its hydrophobic nature [10]. Moreover, the results show that modified Nafion[®] nanocomposite membranes can maintain mechanical strength when operating in high temperature fuel cell applications, as their secant modulus is higher at dry state than wet state. The incorporation of ZrO₂ nanoparticles within Nafion[®] membrane has resulted in an increase in secant modulus [18, 19]. This may be due to the free motion within the membrane chains that was slightly restricted by intermolecular forces between the membrane chains and inorganic oxide nanoparticles.

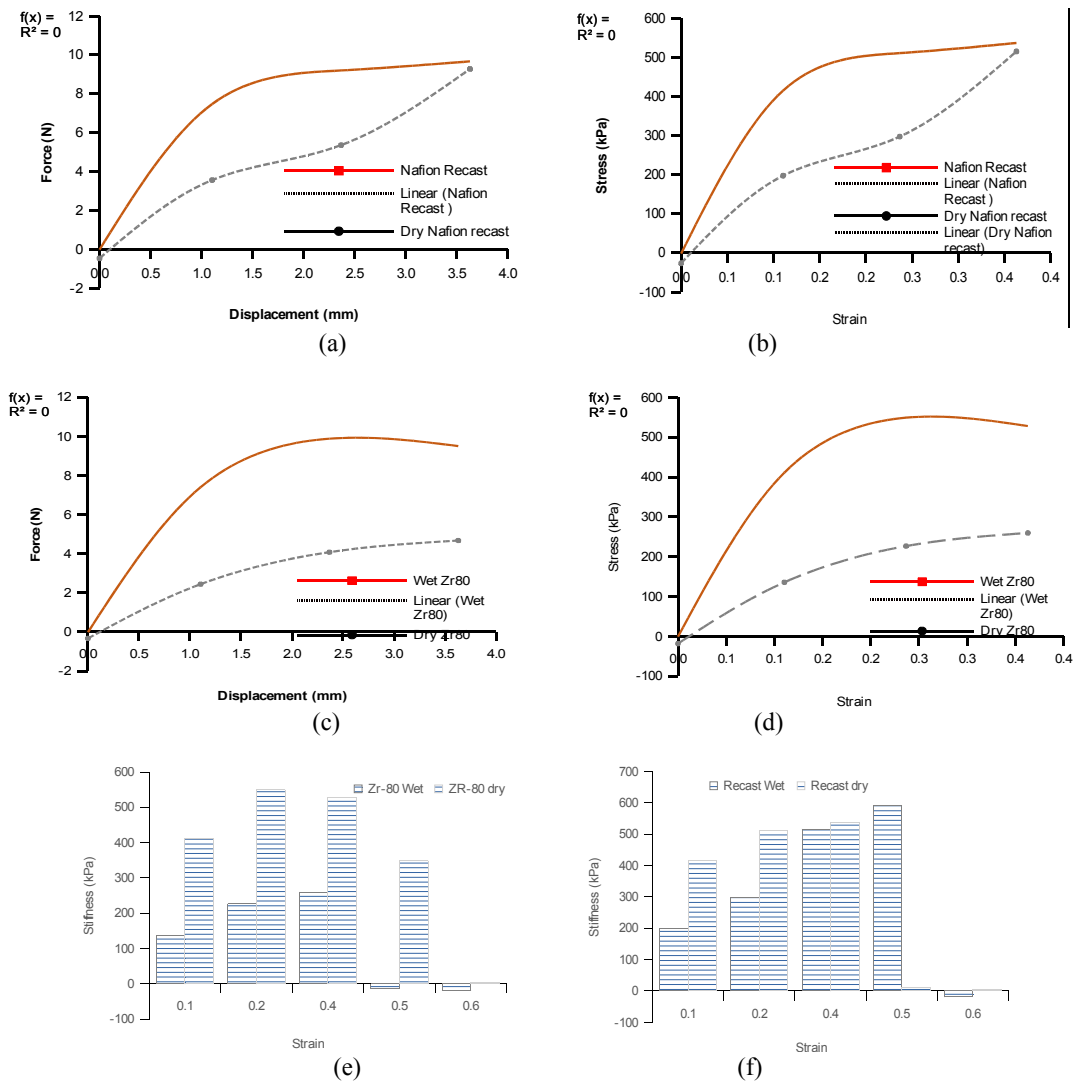


Fig. 4. Mechanical tensile tests results of recast Nafion[®] and Nafion[®]/ Zr-80 nanocomposite membranes show (a) the stiffness of dry and wet recast Nafion[®], (b) the elastic modulus of dry and wet recast Nafion[®], (c) the stiffness of dry and wet Nafion[®]/ Zr-80 nanocomposite membrane and (d) the elastic modulus of dry and wet of Nafion[®]/ Zr-80 nanocomposite membrane, Secant modulus of dry and wet (e) Nafion[®]/Zr-80, (f) Recast-

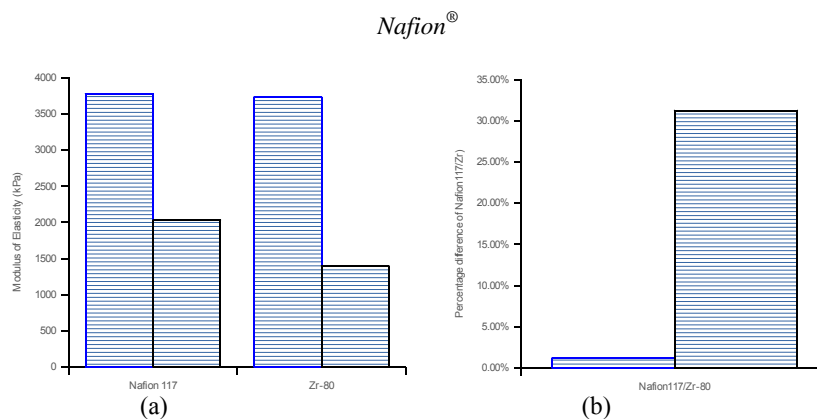


Fig. 5. Comparison of modulus of elasticity (a) dry and wet recast *Nafion*[®] and *Nafion*[®]/Zr-80 nanocomposite membranes and (b) dry/wet recast *Nafion*[®] and dry/wet *Nafion*[®]/Zr-80 nanocomposite membranes

3.4. Structure analysis

The structure of zirconia nanoparticles, nanocomposite membranes and recast *Nafion*[®] was measured by X-ray diffraction (XRD) as shown in Figure 6(a-c). Figure 6(a) shows that the crystallinity of zirconia nanoparticles resemble diffraction patterns corresponding to the cubic phase (JCPDS No. 65-1022). The diffraction peaks at 2θ are 30.2° , 35.2° , 50.6° , 60.2° , 74.2° and 82.5° which correspond to the planes (1 1 1), (2 0 0), (2 2 0), (3 1 1), (4 0 0), (3 3 1) [41, 42]. Corresponding to d-spacing of 0.51291 nm (a-c) and $\beta = 90.0^\circ$, cubic phase ZrO_2 nanoparticles were spectra indexed. Figure 6(b) shows that the recast *Nafion*[®] membrane consisted of two diffractions peaks at 17.5° and 39° 2θ which resemble the crystallinity in the perfluorocarbon chains of the ionomer [43]. It is noticeable in Figure 6(c) that ZrO_2 nanoparticles are well distributed on surface moieties of recast *Nafion*[®] membrane, as the entire *Nafion*[®] peak at 17.5° and 39° 2θ has disappeared. Only observed ZrO_2 peaks within the composite membrane showing the existence of nanoparticles within the membrane, matching Figure 5(a) perfectly. The diffraction peaks at 2θ are 30.2° , 35.2° , 50.6° , 60.2° , 74.2° and 82.5° which correspond to the planes (1 1 1), (2 0 0), (2 2 0), (3 1 1), (4 0 0), (3 3 1) [41, 42]. Moreover, it can be observed in Figure 6(c) that the introduction of ZrO_2 nanoparticles decreases the crystallinity of *Nafion*[®] membrane [44].

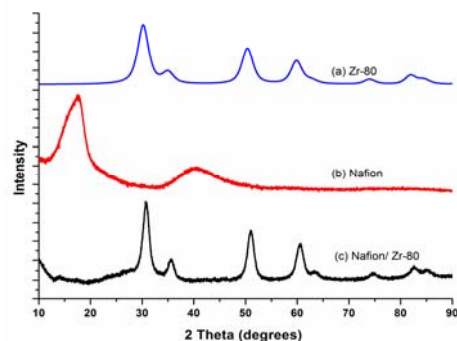


Fig. 6. XRD patterns of Zr-80 nanoparticles (a), recast *Nafion*[®] membrane (b) and *Nafion*[®]/Zr-80 nanocomposite membrane (c)

3.5. Degradation at High Temperatures

Thermal degradation of a composite membrane compared to recast *Nafion*[®] was observed under thermal gravimetric analysis (TGA) and Fourier transform infrared spectroscopy (FT-IR).

3.5.1. Thermo-gravimetric analysis (TGA)

The thermal degradation of nanocomposite membrane, zirconia nanoparticles, was compared to recast Nafion[®] and observed under thermal gravimetric analysis (TGA) in Figure 7. Figure 7(a) shows that Zr-80 lost little of its original weight when heated to 100 °C. Any weight loss is attributed to the removal of adsorbed water on the surface [45]. The second weight loss occurs between 100 °C and 900 °C and corresponds to the removal of terminal hydroxyl groups bonded to the surface of zirconia [45]. Zr-80 lost 8% of its total weight mass with less decomposition of oxide. Figure 7(b) shows that the modified Nafion[®] membrane with zirconia nanoparticles has more thermal stability compared to recast Nafion[®] membrane that completely lost weight, the same finding obtained by other researchers [46]. This may be due to water retention of inorganic additives within the membrane that interact closely with the hydrophobic backbone of Nafion[®] membrane [47, 48]. Moreover, Figure 7 (b) shows that modified nanocomposite membrane has better thermal properties than recast Nafion[®] membrane as it started to decompose at 530 °C, whereas the recast Nafion[®] membrane started to decompose at 360 °C. Some researchers report that the sulfonic acid group of pure Nafion[®] membrane begins to decompose at 280 °C [49, 50]. Figure 7(b-c), shows that all the membranes undergo three weight loss stages; initial weight loss due to the evaporation of hydrated water, a second weight loss due to the decomposition of the sulfonic acid groups of Nafion[®] membrane [51], while the third is due to degradation and combustion of the polymer main chain [18, 32, 52]. As expected, recast Nafion[®] membrane in Figure 7(c) degrades faster in all stages when compared to a modified membrane. The improvement in thermal stability shows the possibility of modified membranes functioning in the high temperature PEMFCs and low relative humidity, due to the inorganic nanofiller that contributes to the water retention at high temperatures [18].

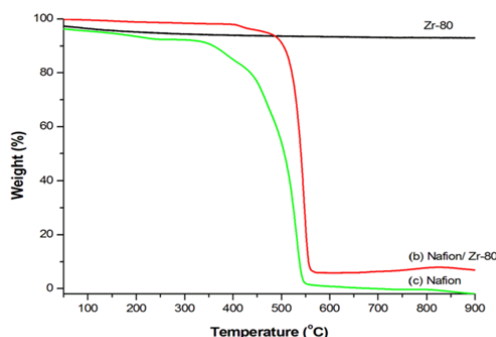


Fig. 7. Thermograms of Zr-80 nanoparticles (a), Nafion/ Zr-80 nanocomposite membrane (b) and recast Nafion membrane (c)

3.5.2. FT-IR analysis

The degradation of the nanocomposite membrane, zirconia nanoparticles and recast membrane was investigated by FT-IR as shown in Figure 8. Figure 8(a), shows vibration bands at 863 cm^{-1} and 926 cm^{-1} are due to Zr-O vibration [53], the peak at 1393 cm^{-1} and 1434 cm^{-1} are assigned to O-H bonding, while the peak observed at 2346 cm^{-1} is due to the presence of inorganic ions. Figure 8(b) shows that the nanocomposite membrane clearly exhibited a broad peak at a wavenumber of 3480 cm^{-1} which corresponds to the presence of bound water and the -OH functional group on the surface of the Zr nanoparticles. The water that tightly bound the surface of the Zr nanoparticles resulted in it being highly stable at temperatures greater than 100 °C. Figure 8(b) shows a vibration peak at 1016 cm^{-1} that could be attributed to vibrational mode of Zr-O and a peak at 1550 cm^{-1} due to Zr-OH bending vibrations, indicating the presence of zirconia nanoparticles within the modified Nafion membrane [54]. Figure 8(c) shows that the O-H vibration of physically adsorbed water occurs at wavenumbers of 3451 cm^{-1} and 3456 cm^{-1} [55,

56]. Figure 8(b-c), shows vibration peaks at 1195 cm^{-1} and 1198 cm^{-1} attributed to the $-\text{CF}_2-\text{CF}_2-$ vibration, and at 1060 cm^{-1} attributed to $-\text{SO}_3^-$ [49, 57].

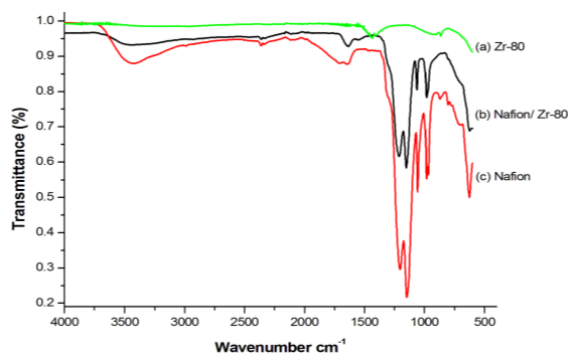


Fig. 8. FTIR spectra of Zr-80 nanoparticles (a), Nafion/ Zr-80 nanocomposite membrane (b) and recast Nafion membrane (c)

3.6. Water contact angle and water uptake Measurement

One very important element that determines the performance of the PEMFC is the water-content dependence of the protonic conductivity in the ionomer membrane. The contact angle was measured to determine the effect of ZrO_2 nanoparticles on the hydrophilicity and hydrophobicity of modified membranes. The digital images of water droplets at the surface area of recast Nafion[®] and modified membrane are presented in Figure 9 below. Figure 9 (a-b) shows the modified Nafion[®] membrane with Zr-80 nanoparticles acts as a hydrophilic surface as the obtained contact angles are less than 90° whereas the recast Nafion[®] membrane is hydrophobic surface since it obtained the contact angle above 90° as indicated in Figure 9 (c-d). Generally, the contact angles of the modified membranes decreased from 88° to 64° when compared with those of unmodified recast Nafion[®] membranes (118° to 100°). This may due to the hydrophilicity of nanoparticles adsorbed on the surface of membrane [58]. Contact angles below 90° indicate the hydrophilic character of a sample describing the water-uptake capability. Figure 8 (d) shows that when a water droplet touches the hydrophobic recast Nafion membrane, its morphological structure immediately changes as it swells within the measured time [59]. In contrast, Figure 9(b) shows no swelling of the membrane, due to the incorporation of inorganic anti-swelling oxide nanoparticles within the membrane matrix [12-15]. Figure 9(e) shows the water uptake percentage of modified membrane and recast Nafion[®] membrane. In Figure 9(e), we find that the modified Nafion membrane with inorganic filler of zirconium oxide has obtained a higher water uptake of 34 % when compared to recast Nafion membrane (30%), this may be due to inorganic fillers distributed on the pores of swollen membranes increasing the hydrophilic nature of Nafion [60]. Incorporating zirconia nanoparticles with higher porosity increases water retention within the nanocomposite membranes which in turn increases exchange sites per cluster and proton conductivity, an important parameter of fuel cells operating at higher temperatures [61].

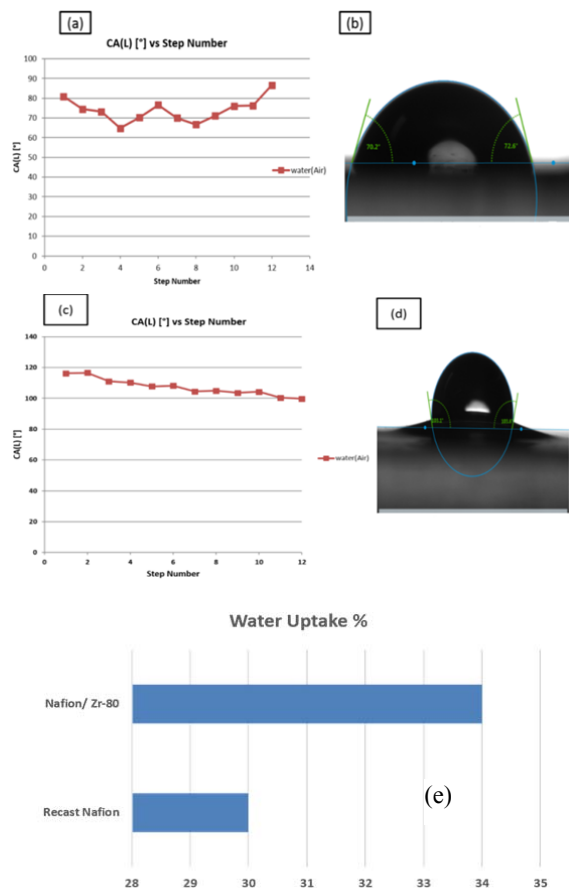


Fig. 9. Water contact angle of Nafion[®]/Zr-80 nanocomposite (a-b) and recast Nafion[®] membranes (c-d), Water uptake of Nafion[®]/Zr-80 nanocomposite and recast Nafion[®] membranes (e)

4. Conclusions

The modified membranes obtained by recast method show a decrease in water contact angle when compared to the recast Nafion[®] membrane. Furthermore, the water uptake of modified membrane is higher than that of recast Nafion[®] membrane, which may be due to the incorporation of the inorganic nanofiller that adsorbs water. XRD, AFM and SEM results show that using zirconia nanoparticles as an inorganic filler improves the morphology and crystallinity of Nafion[®] membranes, as it was well dispersed within the Nafion matrix making them suitable candidates for fuel cell applications.

The incorporation of zirconia nanoparticles also shows the effect on hydrophilicity roughness of the membrane. The strength of Nafion[®]/Zr-80 nanocomposite membrane in its wet state was greatly affected by moisture content when compared to recast Nafion[®] membrane. However, obtained results show that modified Nafion[®] nanocomposite membranes can maintain mechanical strength when operating in high temperature fuel cells, as their secant modulus is higher at dry state than wet state. The incorporation of ZrO₂ nanoparticles within the Nafion[®] membrane has resulted in an increase in secant modulus. TGA results show zirconia nanoparticles improved the thermal stability of the modified membrane when compared to recast Nafion[®] membrane. In addition, the modified membrane started decomposing at a higher temperature when compared to the pure recast Nafion[®] membrane.

Acknowledgment

The authors would like to acknowledge and thank the National Research Foundation of South Africa and University of South Africa (AQIP) for their financial support. We are also thankful to Dr James Wesley-Smith (CSIR) for the SEM results.

References

- [1] K. Ketpang, B. Son, D. Lee, S. Shanmugam, *Journal of Membrane Science* **488**, 154 (2015).
- [2] T. Xiangguo, D. Jicui, S. Jing, *Journal of Solid State Electrochemistry* **19**(4), 1091 (2015).
- [3] V. Vishnyakov, *Vacuum* **80**(10), 1053 (2006).
- [4] K. Kreuer, *Journal of Membrane Science* **185**(1), 29 (2001).
- [5] T. Gierke, G. Munn, F. Wilson, *Journal of Polymer Science: Polymer Physics Edition* **19**(11), 1687 (1981).
- [6] L. A. Zook, J. Leddy, *Analytical chemistry* **68**(21), 3793 (1996).
- [7] W. Zhengbang, H. Tang, P. Mu, *Journal of Membrane Science* **369**(1), 250 (2011).
- [8] A. Sacca, I. Gatto, A. Carbone, R. Pedicini, E. Passalacqua, *Journal of power sources* **163**(1), 47 (2006).
- [9] M. A. Dresch, R. A. Isidoro, M. Linardi, J. F. Q. Rey, F. C. Fonseca, E. I. Santiago, *Electrochimica Acta* **94**, 353 (2013).
- [10] M. B. Satterfield, P. W. Majsztrik, H. Ota, J. B. Benziger, A. B. Bocarsly *Journal of Polymer Science Part B: Polymer Physics* **44**(16), 2327 (2006).
- [11] E. Chalkova, M. B. Pague, M. V. Fedkin, D. J. Wesolowski, S. N. Lvov, *Journal of The Electrochemical Society* **152**(6), A1035 (2005).
- [12] A. C. Brown, J. J. Hargreaves, *Green Chemistry* **1**(1), 17 (1999).
- [13] Y. Lu, Y. Yang, A. Sellinger, M. Lu, J. Huang, H. Fan, R. Haddad, G. Lopez, A. R. Burns, D. Y. Sasaki, *Nature* **410**(6831), 913 (2001).
- [14] C.-C. Yang, Y. J. Li, T.-H. Liou, *Desalination* **276**(1), 366 (2011).
- [15] M. A. Zulfikar, A. W. Mohammad, N. Hilal, *Desalination* **192**(1-3), 262 (2006).
- [16] S. Licoccia, E. Traversa, *Journal of power sources* **159**(1), 12 (2006).
- [17] M. R. H. Siddiqui, A. I. Al-Wassil, A. M. Al-Otaibi, R. M. Mahfouz, *Materials Research*, **15**(6), 986 (2012).
- [18] K. T. Adjemian, R. Dominey, L. Krishnan, H. Ota, P. Majsztrik, T. Zhang, J. Mann, B. Kirby, L. Gatto, M. Velo-Simpson, *Chemistry of materials* **18**(9), 2238 (2006).
- [19] N. H. Jalani, K. Dunn, R. Datta, *Electrochimica Acta* **51**(3), 553 (2005).
- [20] S. Lu, D. Wang, S. P. Jiang, Y. Xiang, J. Lu, J. Zeng, *Advanced Materials* **22**(9), 971 (2010).
- [21] Z. Chen, B. Holmberg, W. Li, X. Wang, W. Deng, R. Munoz, Y. Yan, *Chemistry of Materials* **18**(24), 5669 (2006).
- [22] B. Bonnet, D. Jones, J. Roziere, L. Tchicaya, G. Alberti, M. Casciola, L. Massinelli, B. Bauer, A. Peraio, E. Ramunni, *Journal of New Materials for Electrochemical Systems* **3**(2), 87 (2000).
- [23] A. B. Yaroslavtsev, V. V. Nikonenko, V. I. Zabolotsky, *Russian chemical reviews* **72**(5), 393 (2003).
- [24] T. Xu, *Journal of membrane science* **263**(1), 1 (2005).
- [25] J. Yang, P. K. Shen, J. Varcoe, Z. Wei, *Journal of Power Sources* **189**(2), 1016 (2009).
- [26] M. Navarra, F. Croce, B. Scrosati, *Journal of Materials Chemistry* **17**(30), 3210 (2007).
- [27] K. Wang, L. Chen, J. Wu, M. L. Toh, C. He, A. F. Yee, *Macromolecules* **38** (3), 788 (2005).
- [28] T. Fornes, D. Paul, *Polymer* **44**(14), 3945 (2003).
- [29] M. Munoz, S. Gallego, J. Beltrán, J. Cerdá, *Surface Science Reports* **61**(7), 303 (2006).
- [30] V. Grover, R. Shukla, A. Tyagi, *Scripta materialia* **57**(8), 69902 (2007).
- [31] W. Li, H. Huang, H. Li, W. Zhang, H. Liu, *Langmuir* **24**(15), 8358 (2008).
- [32] Y. Zhai, H. Zhang, J. Hu, B. Yi, *Journal of membrane science* **280**(1), 148 (2006).
- [33] H. Yu, C. Ziegler, M. Oszcipok, M. Zobel, C. Hebling, *Electrochimica Acta* **51**(7), 1199 (2006).

- [34] K. Matsui, M. Ohgai, *Journal of the American Ceramic Society* **84**(10), 2303 (2001).
- [35] F. Bauer, M. Willert-Porada, *Journal of Membrane Science* **233**(1), 141 (2004).
- [36] G. M. K. Tolba, A. M. Bastaweesy, E. A. Ashour, W. Abdelmoez, K. A. Khalil, N. a. M. Barakat, *Arabian Journal of Chemistry* **9**(2), 287 (2016).
- [37] A. Lehmani, S. Durand-Vidal, P. Turq, *Journal of applied polymer science* **68**(3), 503 (1998).
- [38] P. James, J. Elliott, T. McMaster, J. Newton, A. Elliott, S. Hanna, M. Miles, *Journal of Materials Science* **35**(20), 5111 (2000).
- [39] P. Velayutham, A. K. Sahu, S. Parthasarathy, *A Energies* **10**(2), 259 (2017).
- [40] A. Realpe, N. Mendez, M. Acevedo, *International Journal of Engineering and Technology* **6**(5), 2435 (2014).
- [41] M. Tahmasebpour, A. Babaluo, M. R. Aghjeh, *Journal of the European Ceramic Society* **28**(4), 773 (2008).
- [42] F. Davar, A. Hassankhani, M. R. Loghman-Estarki, *Ceramics International* **39**(3), 2933 (2013).
- [43] H. W. Starkweather Jr, *Macromolecules* **15**(2), 320 (1982).
- [44] A. V. Penkova, S. F. Acquah, M. E. Dmitrenko, M. P. Sokolova, M. E. Mikhailova, E. S. Polyakov, S. S. Ermakov, D. A. Markelov, D. Roizard, *Materials & Design* **96**, 416 (2016).
- [45] E. Gil, Á. Mas, C. Lerma, J. Vercher, *Advances in Materials Science and Engineering* **2015**, (2015)
- [46] W. Jia, K. Feng, B. Tang, P. Wu, *Journal of Materials Chemistry A* **3**(30), 15607 (2015).
- [47] Y. Devrim, S. Erkan, N. Baç, I. Eroglu, *international journal of hydrogen energy* **37**(21), 16748 (2012).
- [48] J. Pan, H. Zhang, W. Chen, M. Pan, *international journal of hydrogen energy* **35**(7), 2796 (2010)
- [49] Y. Zhai, H. Zhang, J. Hu, B. Yi, *Journal of Membrane Science* **280**(1), 148 (2006).
- [50] G. Gupta, S. Sharma, P. Mendes, *RSC advances* **6**(86), 82635 (2016).
- [51] T. Kyu, M. Hashiyama, A. Eisenberg, *Canadian Journal of Chemistry* **61**(4), 680 (1983).
- [52] B. Smitha, D. A. Devi, S. Sridhar, *international journal of hydrogen energy* **33**(15), 4138 (2008)
- [53] M. Jansen, E. Guenther, *Chemistry of materials* **7**(11), 2110 (1995).
- [54] D. Sarkar, D. Mohapatra, S. Ray, S. Bhattacharyya, S. Adak, N. Mitra, *Ceramics International* **33**(7), 1275 (2007).
- [55] V. Baglio, A. Di Blasi, V. Antonucci, *Electrochemistry communications* **5**(10), 862 (2003).
- [56] H. Yang, D. Lee, S. Park, W. Kim, *Journal of membrane science* **443**, 210 (2013).
- [57] J. Ostrowska, A. Narebska, Part 1, *Colloid and Polymer Science* **261**(2), 93 (1983).
- [58] Y. Xuesong, REMOVED: Preparation, Characterization and Application of a Novel PA/SIO₂ NF Membrane, *Procedia Engineering* **44**, 2075 (2012).
- [59] L. Zou, I. Vidalis, D. Steele, A. Michelmore, S. Low, J. Verberk, *Journal of membrane Science* **369**(1), 420 (2011).
- [60] O. Savadogo, *Journal of New Materials for Electrochemical Systems* **1**(1), 47 (1998).
- [61] T. A. Zawodzinski, C. Derouin, S. Radzinski, R. J. Sherman, V. T. Smith, T. E. Springer, S. Gottesfeld, *Journal of the Electrochemical Society* **140**(4), 1041 (1993).